Evaluation of Diimine Ligand Exchange on Cu(I)

Elvira Riesgo, Yi-Zhen Hu, Frédéric Bouvier, and Randolph P. Thummel*

Department of Chemistry, University of Houston, Houston, Texas 77204-5641

Received January 18, 2000

Four ligands have been prepared, 8,8-dimethyl-6,7,9-trihydropyrido[1,2-*b*]acridine and three 4,4′,6,6′-tetrasubstituted derivatives of 2,2′-bipyrimidine where the substituents are methyl, phenyl, and *p*-tolyl. The corresponding $[CuL_2]^+$ salts of these ligands evidence nonequivalent NMR signals that allow an estimation of the ligand exchange barrier in both acetonitrile and chloroform solution. Lower barriers are found in the former solvent and attributed to solvent participation in the exchange process. Corresponding differences in the oxidation potentials of the complexes are explained in a similar manner. The electronic absorption properties of the complexes are also consistent with the steric and electronic properties of the ligands. $[Cu(\mathbf{2c})_2](PF_6)$, where **2c** = 4,4′,6,6′-tetraphenyl-2,2′-bipyrimidine, was analyzed by X-ray diffraction and found to crystallize in the space group *Pccn* with $a = 14.761(2)$ Å, $b = 15.007(2)$ Å, $c = 24.407(4)$ Å, and $Z = 4$. The internal and external phenyl rings are disposed quite differently, with the internal rings interacting strongly with the orthogonal ligand.

Introduction

Over the past few decades chemists have become increasingly concerned with the employment of metal−ligand interactions in the construction of organized supramolecular assemblies.[1] The Cu(I) ion lends itself particularly well to this task through the formation of bis-diimine complexes with a variety of judiciously designed bridging ligands. The advantage of these systems stems from their preference for tetrahedral geometry, allowing ligands to be oriented in orthogonal planes, and the kinetic lability of the Cu(I) complexes which allows ligand−metal exchange to occur readily in solution. Formation of the thermodynamically favorable, and readily predictable, complex often results.

An early example of molecular architecture involving Cu(I) was the "molecular box" constructed by Osborn and Youinou.[2] The bridging ligand, 3,6-di(2′-pyridyl)pyridazine, assembles around four Cu(I) centers to afford the box, which is the simplest arrangement of the ligand and metal that allows every binding site on both species to be occupied without undue distortion. Interestingly, stabilizing π-stacking interactions between the ligands may also assist in the assembly process.[3] Baxter, Lehn, and co-workers have exploited this self-assembly theme using a variety of polypyridine bridging ligands as well as an assortment of metals. The construction of rods,[4] ladders,[5] and larger grids[6] has emphasized the importance of facile metal−ligand exchange.

Albrecht-Gary and co-workers have recently explored the importance of steric and electronic effects on the stability of mono- and bischelate Cu(I) complexes of 2,9-disubstituted derivatives of 1,10-phenanthroline.[7] Insights were gained primarily through cyanide-assisted demetalation kinetic studies. We have examined the Cu(I) complexes of a series of 2,2′-biquinolines where the biquinoline could be replaced by the stronger binding 2,9-dimethyl-1,10-phenanthroline.[8] This exchange could be monitored spectrophotometrically, but, due to complexities imposed by the involvement of partially exchanged intermediates, these systems did not allow a quantitative assessment of the ligand exchange barrier. This paper will examine several ligand systems which do allow an estimate of this exchange barrier, and the effects of structure and solvent will be discussed.

For $[Cu(L)_2]^+$ complexes, where L is an unsymmetrical diimine-type ligand, stereoisomers are possible at the metal center.[9] This chirality at Cu(I) creates a situation where geminal groups on the cyclohexeno ring of **1a** become diastereotopic in the corresponding complex $[Cu(\mathbf{1a})_2]^+$. Thus, one should be able to observe independent ^{1}H NMR resonances for such geminal protons. In practice, the chemical shift difference between these geminal protons is too small to allow clear resolution and interpretation. If one introduces a pair of geminal methyl groups as in **1b**, however, their ^{1}H resonances should be more readily distinguishable, depending on the integrity of the complex. Where ligand exchange is rapid on the NMR time scale, only

(1) Lehn, J.-M. *Supramolecular Chemistry: Concepts and Perspectives*, VCH: 1995, Chapter 9.
(2) Youinou, M.-T.; Rahmouni, N.; Fischer, J.; Osborn, J. A. *Angew. Chem., Int. Ed. Engl.* **1992**, *31*, 733.
(3) Riesgo, E. C.; Bouvier, F.; Thummel, R. P. *Inorg. Chem.*, in press.
(4) (a) Wärnmark, K.; Baxter, P. N. W.; Lehn, J.-M. *Chem. Commun. (Cambridge)* **1998**, 993. (b) Sleiman, H.; Baxter, P. N. W.; Lehn, J.-M.; Airola, K.; Rissanen, K. *Inorg. Chem.* **1997**, *36*, 4734. (c) Sleiman, H.; Baxter, P. N. W.; Lehn, J.-M.; Rissanen, K. *J. Chem. Soc., Chem. Commun.* **1995**, 715.
(5) (a) Baxter, P. N. W.; Hanan, G. S.; Lehn, J.-M. *Chem. Commun. (Cambridge)* **1996**, 2019. (b) Baxter, P.; Lehn, J.-M.; De Cian, A.; Fischer, J. *Angew. Chem., Int. Ed. Engl.* **1993**, *32*, 69.
(6) (a) Baxter, P. N. W.; Lehn, J.-M.; Kneisel, B. O.; Fenske, D. *Chem. Commun. (Cambridge)* **1997**, 2231. (b) Baxter, P. N. W.; Lehn, J.-M.; Kneisel, B. O.; Fenske, D. *Angew. Chem., Int. Ed. Engl.* **1997**, *36*, 1978. (c) Baxter, P. N. W.; Lehn, J.-M.; Rissanen, K. *Chem. Commun. (Cambridge)* **1997**, 1323. (d) Baxter, P.; Lehn, J.-M.; Fischer, J.; Youinou, M.-T. *Angew. Chem., Int. Ed. Engl.* **1994**, *33*, 2284.
(7) Meyer, M.; Albrecht-Gary, A.-M.; Dietrich-Buchecker, C. O.; Sauvage, J.-P. *Inorg. Chem.* **1999**, *38*, 2279.
(8) Jahng, Y.; Hazelrigg, J.; Kimball, D.; Riesgo, E.; Wu, F.; Thummel, R. P. *Inorg. Chem.* **1997**, *36*, 5390.
(9) Riesgo, E. C.; Credi, A.; De Cola, L.; Thummel, R. P. *Inorg. Chem.* **1998**, *37*, 2145.

10.1021/ic0000606 CCC: $20.00
Published on Web 04/20/2001

one signal will be observed, while slow exchange should evidence a separate peak for each methyl group.

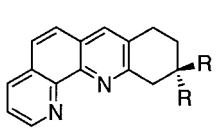

1 a R = H
b R = CH_3

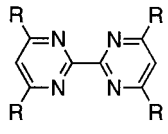

2 a R = H
b R = CH_3
c R = C_6H_5
d R = *p*-tolyl

A related series of ligands which shows symmetry differences in the complexed and uncomplexed states are the 2,2′-bipyrimidines **2a**−**d**. In the free ligand, substituents at the 4,4′- and 6,6′-positions will be equivalent, but when two ligands are bound in a tetrahedral fashion to a single metal, one pair of these substituents points in toward the metal and one points away, making them nonequivalent and potentially distinguishable by ^{1}H NMR.

Results and Discussion

The phenanthrolines **1a**,**b** were prepared in a straightforward fashion by the Friedländer condensation of 8-amino-7-quinolinecarbaldehyde (**3**)[10] with either cyclohexanone or 3,3-dimethylcyclohexanone. It is noteworthy that, in the latter reaction, only the 8,8-dimethyl isomer is formed to the total exclusion of the 6,6-dimethyl species. To obtain the 6,6-dimethyl isomer would have required that the enamine, initially formed between **3** and **4b**, subsequently condense at the much more hindered 2-position of **4b**.

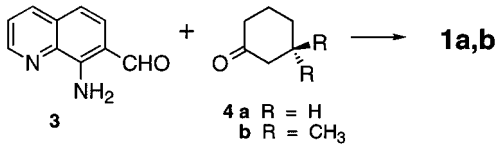

3 **4 a** R = H
b R = CH_3

The parent 2,2′-bipyrimidine (**2a**) was commercially available; however, it was suspected that complexation-induced differences between the 4,4′- and 6,6′-protons might be difficult to discern. Such differences should be more apparent for the substituted derivatives **2b**−**d** which were all prepared by a Ni(0)-promoted coupling[11] of the corresponding 2-chloropyrimidine. The tetra-*p*-tolylbipyrimidine **2d**, which has not previously been reported, was prepared in three steps from diketone **5**.

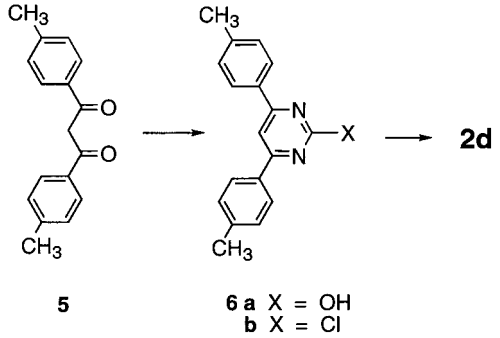

5 **6 a** X = OH
b X = Cl

The ligands **1a**,**b** and **2b**−**d** were treated with either $[Cu(CH_3CN)_4](ClO_4)$ or $[Cu(CH_3CN)_4](PF_6)$ in acetonitrile to afford the corresponding $[Cu(L)_2]^+$ salt in good yield. These complexes were readily characterized by their ^{1}H NMR spectra. For the complex of **1b**, the aliphatic region of the NMR is displayed in Figure 1 and clearly shows three well-resolved methylene signals. At 3.14 ppm a triplet appears for H6. The adjacent non-benzylic H7 shows an upshifted triplet at 1.59 ppm. The H9 protons appear as a singlet at 2.46 ppm, shielded by 0.73 ppm due to proximity of the Cu(I) center.

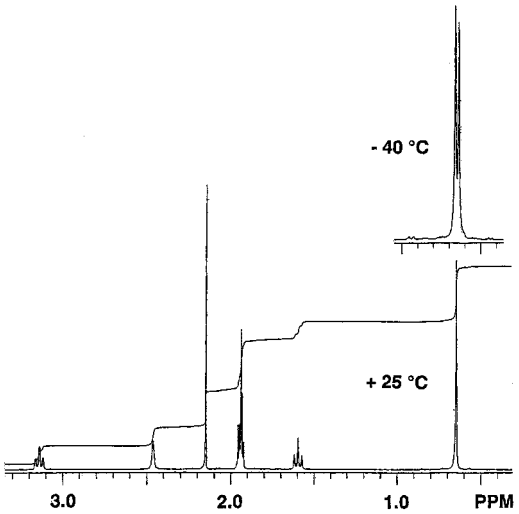

Figure 1. Upfield region of the 300 MHz ^{1}H NMR of $[Cu(\mathbf{1b})_2](ClO_4)$ in CD_3CN (δ 1.94, H_2O: δ 2.15).

Table 1. Ligand Exchange Data for Cu(I) Complexes Studied by VT NMR[a]

complex	T_c (±2 K)	k_c (s^{-1}, ±20%)	$\Delta G^{\ddagger}$ (±0.2 kcal/mol)
		CD_3CN	
$[Cu(\mathbf{1b})_2](ClO_4)$	265[b]	15	14
$[Cu(\mathbf{2b})_2](PF_6)$	248[b]	313	11.6
$[Cu(\mathbf{2c})_2](PF_6)$	273[c]	344	12.8
$[Cu(\mathbf{2d})_2](PF_6)$	288[c]	350	13.5
		$CDCl_3$[d]	
$[Cu(\mathbf{1b})_2](ClO_4)$	283[b]	11	15.2
$[Cu(\mathbf{2d})_2](PF_6)$	318[b]	510	14.7
	318[c]	528	14.7

[a] Calculated at the coalescence temperature T_c according to $\Delta G^{\ddagger} = 4.58T_c[10.32 + \log(T_c/k_c)]$ cal/mol, where k_c (ligand exchange rate) = $(\pi \times \Delta\upsilon)/\sqrt{2}$ and $\Delta\upsilon$ is the peak separation in the absence of exchange. [b] Based on coalescence of CH_3 signals. [c] Based on coalesence of Ar−H signals. [d] Peaks for **2b** complex were too broad and there was insufficient sample of **2c** complex.

The complexes of **1b** and **2b**−**d** were then analyzed at various temperatures in acetonitrile-d_3 and chloroform-*d* to determine the coalescence temperature for their diastereotopic NMR signals. For $[Cu(\mathbf{1b})_2](ClO_4)$ in CD_3CN at 25 °C, the geminal methyl groups of **1b** evidence a sharp singlet at 0.65 ppm. Upon cooling to −40 °C, the ligand exchange becomes sufficiently slow such that the two diastereotopic methyl groups become clearly resolved (Figure 1). The methylene signals, however, remain essentially unchanged. A similar effect is observed for the 4,4′,6,6′-substituents on the bipyrimidine ligands in complexes of **2b**−**d**. The observed coalescence temperatures and resulting exchange rate and free energy change data are collected in Table 1. It is noteworthy that, for $[Cu(\mathbf{2d})_2](PF_6)$, the $\Delta G^{\ddagger}$ value is identical when either the methyl or aryl protons of the *p*-tolyl group are monitored.

The ligand exchange barriers in acetonitrile fall within the fairly narrow range of 11.6−14.0 kcal/mol. Three interesting

(10) Riesgo, E. C.; Jin, X.; Thummel, R. P. *J. Org. Chem.* **1996**, *61*, 3017.
(11) (a) Tiecco, M.; Testaferri, L.; Tingoli, M.; Chianelli, D.; Montanucci, M. *Synthesis* **1984**, 736. (b) Semmelhack, M. F.; Helquist, P. M.; Jones, L. D. *J. Am. Chem. Soc.* **1971**, *93*, 5908.

and self-consistent effects are in evidence. First, we can correlate binding strength with ligand basicity. With four nitrogens, 2,2′-bipyrimidine ($pK_a = 0.6$) is considerably less basic than 1,10-phenanthroline ($pK_a = 5.2$)[12] and thus should form a weaker coordinative bond, explaining its lower exchange barriers as compared to **1b**. Part of this difference may also be due to the flexibility of bipyrimidine about the 2,2′-bond which should facilitate its stepwise coordination and decoordination.

For the two systems which could be clearly measured in both solvents, we observe that, in both cases, the barrier is 1.3 kcal/mol higher in chloroform than in acetonitrile. This observation is consistent with the fact that the latter is a stronger coordinating solvent and thus can facilitate ligand exchange. It seems likely that the exchange process will be assisted by solvent binding to partially exchanged intermediate species. Frei and Geier have similarly observed that ligand exchange for $[Cu(biq)_2]^+$ (biq = 2,2′-biquinoline) occurs more rapidly in acetonitrile than in acetone or methanol.[13]

Finally, if we examine the series $[Cu(\mathbf{2b}-\mathbf{d})_2]^+$ in acetonitrile, the exchange barrier increases 1.2 kcal/mol in going from the tetramethyl- to the tetraphenyl-substituted bipyrimidine. This barrier increases an additional 0.7 kcal/mol when *p*-tolyl replaces phenyl. If solvent coordination is important to the ligand exchange process, as the size of the substituents on the 2,2′-bipyrimidine is increased, these substituents will interfere to a greater extent with solvent coordination and exchange will become more difficult.

One can test the relative binding strengths of the ligands examined in this study by a competitive exchange experiment. In principle, more weakly binding ligands should be replaced by more strongly binding ones and judicious use of this knowledge could result in the construction of predictable self-assembled arrays. The relative affinities of **1b** and **2b** for Cu(I) can be estimated from the data in Table 1. Considering that the exchange rate k_c will increase as the temperature is raised, we predict that ligand **2b** will exchange much more rapidly than **1b** and thus should be replaced by this species. This prediction was borne out by an experiment in which 2 equiv of the free ligand **1b** was added to a CD_3CN solution of $[Cu(\mathbf{2b})_2]^+$. The NMR spectrum showed the complete disappearance of signals for **1b**, with the appearance of uncomplexed **2b** and $[Cu(\mathbf{1b})_2]^+$.

Being aware that Cu(I) complexes are capable of considerable distortion from ideal tetrahedral geometry,[8] we became interested in the possibility of intramolecular π-stacking in the two tetraaryl derivatives $[Cu(\mathbf{2c},\mathbf{d})_2]^+$. The dihedral angle between these aryl groups and the parent pyrimidine will determine the degree of conjugative interaction between these rings, possible steric effects on coordination, and the existence of π-stacking which may exert a stabilizing influence. Thus we undertook a single-crystal X-ray analysis of $[Cu(\mathbf{2c})_2](PF_6)$, and a drawing of the cation is illustrated in Figure 2 and selected geometric features are summarized in Table 2.

The geometry around Cu(I) appears quite normal. The two Cu−N bonds are equal in length and within the range normally associated with such complexes.[14] The N−Cu−N′ bite angles average 81.3°, which is typical and the nonchelating N−Cu−N bonds angles are nearly equal at about 125.2°, indicating that the two ligands occupy essentially perpendicular planes.

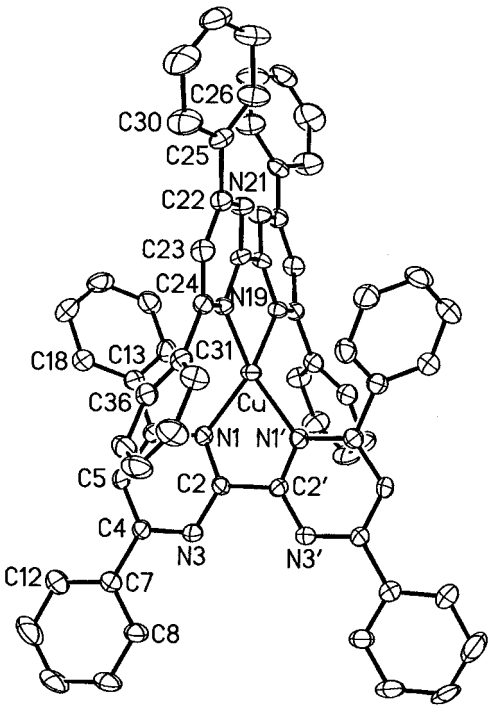

Figure 2. Drawing of the cation of $[Cu(\mathbf{2c})_2](PF_6)$ with atomic numbering scheme.

Table 2. Selected Bond Lengths, Bond Angles, and Dihedral Angles for $[Cu(\mathbf{2c})_2](PF_6)$[a]

Bond Lengths (Å)		Dihedral Angles (deg)	
Cu−N1	2.059(4)	N1−C2−C2′−N1′	22.3(7)
Cu−N19	2.058(4)	N3−C2−C2′−N3′	24.5(7)
		N19−C20−C20′−N19′	21.8(7)
Bond Angles (deg)		N21−C20−C20′−N21′	23.6(7)
N1−Cu−N1′	80.8(2)	N21−C22−C25−C26	15.5(7)
N19−Cu−N19′	81.7(2)	C23−C22−C25−C30	19.9(8)
N1−Cu−N19	125.64(16)	N3−C4−C7−C8	6.3(7)
N1−Cu−N19′	124.70(15)	C5−C4−C7−C12	4.4(8)
N1′−Cu−N19	124.70(15)	N1−C6−C13−C14	47.3(7)
N1′−Cu−N19′	125.64(16)	C5−C6−C13−C18	48.3(7)
		C23−C24−C31−C32	42.9(7)
		N19−C24−C31−C36	44.2(7)

[a] Numbering pattern from Figure 2 with esd's in parentheses.

The bound ligand can evidence rotation about any of its three nonequivalent C−C single bonds, and this rotation is reflected by the dihedral angle between adjacent aryl rings. These dihedral angles may be approximated by the average of two measurements. For the central bipyrimidine, we average N1−C2−C2′−N1′ and N3−C2−C2′−N3′ and find a twist angle of approximately 23.4°. This compares exactly with the angle between the mean planes of the pyrimidines, which also measures 23.4°.

The "internal" and "external" phenyl rings are disposed quite differently, and, especially for the external phenyls, the two ligands are nonequivalent, possibly due to crystal packing forces. One ligand shows an external phenylpyrimidine dihedral angle of 17.4°, and the other shows only 5.4°. Both of these angles are relatively small and indicate that conjugative effects encourage coplanarity of the rings. Figure 2 illustrates that, other than interaction with other molecules in the lattice, the phenyl rings are able to adopt the more favorable coplanar conformation.

The internal phenyls of each ligand interact strongly with the orthogonal ligand and hence rotate about the phenyl−pyrimidine bond to alleviate unfavorable repulsions. We had

(12) Bly, D. D.; Mellon, M. G. *Anal. Chem.* **1963**, *35*, 1386.
(13) (a) Frei, U. M.; Geier, G. *Inorg. Chem.* **1992**, *31*, 187. (b) Frei, U. M.; Geier, G. *Inorg. Chem.* **1992**, *31*, 3132.
(14) (a) Healy, P. C.; Engelhardt, L. M.; Patrick, V. A.; White, A. H. *J. Chem. Soc., Dalton Trans.* **1985**, 2541. (b) Klemens, F. K.; Fanwick, P. E.; Bibler, J. K.; McMillin, D. R. *Inorg. Chem.* **1989**, *28*, 3076. (c) Geoffroy, M.; Wermeille, M.; Buchecker, C. O.; Sauvage, J.-P.; Bernardinelli, G. *Inorg. Chim. Acta* **1990**, *167*, 157.

Table 3. Long-Wavelength Absorption Maxima and Oxidation Potentials for Cu(I) Complexes

		$E_{1/2}$ (ox)[b]	
complex	λ_{max} [a]	CH_3CN	CH_2Cl_2
[Cu(**1a**)$_2$](ClO_4)	458 (0.079)	0.44 (90)	0.65 (256)
[Cu(**1b**)$_2$](ClO_4)	455 (0.061)	0.42 (90)	0.60 (110)
[Cu(**2b**)$_2$](PF_6)	439 (0.045)	0.83 (77)	0.97 (146)
[Cu(**2c**)$_2$](PF_6)	420 (0.064), 544 (0.035)	0.96 (94)	1.10 (82)
[Cu(**2d**)$_2$](PF_6)	420 (0.063), 553 (0.040)	0.87 (83)	1.01 (106)

[a] 10^{-5} M CH_2Cl_2; absorptivities in parentheses. [b] Potentials are in volts vs SCE; solutions were 0.1 M TBAP; $T = 25 \pm 1$ °C; the sweep rate was 200 mV/s; and the number in parentheses is the difference (mV) between the anodic and cathodic waves.

initially expected dihedral angles close to 90° which might lead to π-stacking interactions with the orthogonal pyrimidine. However, these dihedral angles measure 43.6° and 47.8°, averaging near the compromise angle of 45°. It should further be noted that these four phenyl groups quite effectively protect the central copper ion from solvent attack.

An important characteristic of Cu(I) complexes is their oxidative stability. Upon the loss of an electron, the tetrahedral Cu(I) center, in going to Cu(II), becomes approximately square planar and the ligands associated with the metal can have a profound influence on this process. The half-wave oxidation potentials for the complexes being studied are summarized in Table 3 in both acetonitrile and dichloromethane solution. We expect little effect from the substitution of dichloromethane for chloroform as a noncoordinating solvent used in the NMR measurements.

It has been well established for Cu(I) complexes involving ligands related to 2,2′-bipyridine that substituents *ortho* to the chelating nitrogens will stabilize the complex with respect to oxidation by providing steric hindrance to the planarization associated with this process.[15] Interestingly, the 1,10-phenanthroline ring in ligands **1a**,**b** possesses only one such stabilizing substituent, the 2,3-fused cyclohexeno ring. With the other side of the ligand unencumbered, a favorable pathway exists for planarization wherein the two phen rings rotate such that their bulky substituents move apart and do not sterically interfere with each other. The availablity of this oxidative pathway is reflected by the low oxidation potential of +0.42−0.44 V, which is consistent with the value of +0.37 V which we measured for the analogous, and more bulky, 2,3-pinenyl-fused derivative.[9] The bipyrimidine complexes of **2b**−**d** have both their *ortho* positions substituted and hence are considerably more difficult to oxidize with potentials of +0.83−0.96 V. The fact that the more bulky *p*-tolyl derivative oxidizes more readily than the phenyl analogue is somewhat curious and could reflect the slightly better electron-donating ability of the *p*-tolyl group.

There is a solvent effect on the oxidation of these Cu(I) complexes which is consistent with the ligand exchange data discussed earlier. For all the systems studied, oxidation in dichloromethane occurs at higher potential than for acetonitrile, and the waves are much less reversible. For the series [Cu(**2b**−**d**)$_2$]$^+$, an increment of +0.14 V is observed for all three complexes. This difference is attributed to the coordinating ability of acetonitrile which could occupy the apical binding site in the square pyramidal geometry normally associated with the Cu(II) state. It should be noted that Miller and co-workers have suggested that solvent does not bind to the Cu(II) form when it is complexed to a highly congested ligand such as 2,9-diphenyl-1,10-phenanthroline.[16]

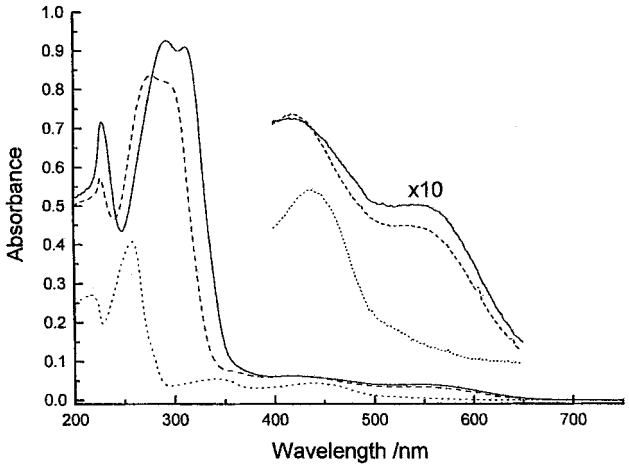

Figure 3. Electronic absorption spectra of [Cu(**2b**)$_2$](PF_6) (···), [Cu(**2c**)$_2$](PF_6) (- - -), and [Cu(**2d**)$_2$](PF_6) (—); 10^{-5} M CH_2Cl_2.

These Cu(I) complexes exhibit a long-wavelength electronic absorption attributed to a metal-to-ligand charge transfer (MLCT) in which the metal is photooxidized in the excited state and an electron is promoted to a vacant π*-orbital on one of the ligands. The electronic absorption data is collected in Table 3. The MLCT transitions have been found to be subject to effects dictated by ligand structure much in the same manner that the redox properties are affected.[17] The two phenanthroline systems [Cu(**1a**,**b**)$_2$]$^+$ show MLCT absorptions at 455−458 nm, which is in the range expected for such systems. Not surprisingly the absorptivity for the unsubstituted derivative **1a** is greater than for the dimethyl derivative **1b**, which would experience a weaker ligand field. The tetramethyl bipyrimidine derivative [Cu(**2b**)$_2$]$^+$ exhibits a slightly higher energy absorption at 439 nm due to the lower basicity of the ligand and its accordingly poorer ability to stabilize the photooxidized state of the metal. Interestingly, the corresponding Ru(II) complexes of **1a** and 1,10-phenanthroline show nearly identical absorption energies,[18] arguing against the importance of ligand basicity in these analogous d_6 complexes.

A second, lower energy band appears at 544 and 553 nm, respectively, for the complexes of the tetraaryl-substituted derivatives **2c**,**d**. Cunningham and co-workers have argued that, for such complexes, the appearance of a pronounced shoulder at about 550 nm suggests considerable distortion of the expected D_{2d} symmetry.[19] Such distortion in the complexes of **2c**,**d** might be attributed to intramolecular $\pi-\pi$ interactions associated with the aryl substituents. The analogous tetramethyl derivative [Cu(**2b**)$_2$]$^+$ shows no long wavelength shoulder (Figure 3). The solid state structure analysis of [Cu(**2c**)$_2$]$^+$ is, however, inconsistent with this explanation, evidencing relatively little distortion from D_{2d} symmetry. Crystal packing forces very likely override the π-stacking effects which may be responsible for distortion in solution. Excitation of CH_2Cl_2 solutions of the complexes under study into their long-wavelength absorption band did not produce any detectable luminescence at room temperature.

(15) (a) Eggleston, M. K.; Fanwick, P. E.; Pallenberg, A. J.; McMillin, D. R. *Inorg. Chem.* **1997**, *36*, 4007. (b) Pallenberg, A. J.; Koenig, K. S.; Barnhart, D. M. *Inorg. Chem.* **1995**, *34*, 2833.

(16) Miller, M. T.; Gantzel, P. K.; Karpishin, T. B. *Inorg. Chem.* **1998**, *37*, 2285.

(17) (a) Miller, M. T.; Gantzel, P. K.; Karpishin, T. B. *Inorg. Chem.* **1999**, *38*, 3414. (b) Eggleston, M. K.; McMillin, D. R.; Koenig, K. S.; Pallenberg, A. J. *Inorg. Chem.* **1997**, *36*, 172.

(18) Juris, A.; Balzani, V.; Barigelletti, F.; Campagna, S.; Belser, P.; von Zelewsky, A. *Coord. Chem. Rev.* **1988**, *84*, 85.

(19) Cunningham, C. T.; Cunningham, K. L. H.; Michalec, J. F.; McMillin, D. R. *Inorg. Chem.* **1999**, *38*, 4388.

In conclusion, we have shown that a judicious choice of ligands can provide a means for estimating the barrier for ligand exchange in Cu(I) diimine type complexes using VT NMR techniques. For two relatively different types of ligands, 1,10-phenanthroline and 2,2′-bipyrimidine, these values span a fairly narrow range of 11.6−14.0 kcal/mol in acetonitrile. This coordinating solvent facilitates ligand exchange as well as oxidation of the complex. Bulky substituents which impede solvent attack lead to higher exchange barriers. The resulting better understanding of the ligand exchange process should assist in the design of more efficient and specific self-assembling ligand−metal complexes. Ideally one can hope for eventual quantification of factors such as ligand basicity, steric bulk, and conformation to allow structure-based predictions of self-assembling tendencies in Cu(I)-based diimine ligand systems. Further efforts are being directed along these lines.

Experimental Section

Nuclear magnetic resonance spectra were recorded on a General Electric QE-300 spectrometer at 300 MHz for ^{1}H NMR and 75 MHz for ^{13}C NMR. Chemical shifts are reported in parts per million downfield from Me_4Si. Electronic spectra were obtained on a Perkin-Elmer 330 spectrophotometer. Mass spectra were obtained on a Hewlett-Packard 5989B mass spectrometer (59987A Electrospray) using the atmospheric pressure ionization (API) method at a temperature of 160 °C for the complexes and atmospheric pressure chemical ionization (APCI) at 300 °C for the ligands. Cyclic voltammograms were recorded using a BAS CV-27 voltammograph or an EG & G Princeton Applied Research Potientiostat/Galvanostat model 263A and a Houston Instruments model 100 X-Y recorder according to a procedure which has been described previously.[20] All solvents were freshly distilled reagent grade. Melting points were measured with a capillary melting point apparatus and are not corrected. Elemental analyses were performed by National Chemical Consulting, Inc., Tenafly, NJ. The 8-amino-7-quinolinecarbaldehyde (**3**),[10] 4,4′,6,6′-tetramethyl-2,2′-bipyrimidine (**2b**),[21] 4,4′,6,6′-tetraphenyl-2,2′-bipyrimidine (**2c**),[22] 1,3-di(*p*-tolyl)-1,3-propanedione (**5**),[23] and $[Cu(CH_3CN)_4]PF_6$ and $[Cu(CH_3CN)_4]ClO_4$[24] were prepared according to literature procedures. ***CAUTION!*** Perchlorate salts of transition metal complexes containing organic ligands are potentially explosive and should be prepared in small quantities and handled with appropriate precautions. While no difficulties were encountered with the complexes reported herein, due caution should be exercised.

6,7,8,9-Tetrahydropyrido[1,2-*b*]acridine (1a). To a solution of cyclohexanone (57 mg, 0.6 mmol) and 8-amino-7-quinolinecarbaldehyde (100 mg, 0.58 mmol) in absolute EtOH (5 mL) was added saturated ethanolic KOH (0.5 mL). The solution was refluxed under Ar for 17 h. The solvent was evaporated, and the residue was chromatographed on alumina (30 g) eluting with CH_2Cl_2/hexane (7:3) to give **1a** (105 mg, 77%) as a beige solid, mp 116−117 °C: ^{1}H NMR ($CDCl_3$) δ 9.32 (d, 1H, J = 3.6 Hz, H_9), 8.38 (d, 1H, J = 7.8 Hz, H_7), 8.01 (s, 1H, H_4), 7.78 (broad s, 2H, H_5/H_6), 7.72 (quartet, 1H, J = 4.5 Hz, H_8), 3.58 (broad s, H_2O), 3.51 (t, 2H, J = 6.3 Hz, $-CH_2$), 3.08 (t, 2H, J = 5.7 Hz, $-CH_2-$), 2.04 (m, 2H, $-CH_2-$), 1.96 (m, 4H, $-CH_2-$); ^{13}C NMR ($CDCl_3$) δ 157.8, 144.4, 135.5, 133.5, 131.4, 127.8, 127.7, 126.8, 125.2, 125.0, 124.4, 124.4, 33.8, 29.2, 23.5, 23.2; MS *m*/*e* 235 (MH^+).

8,8-Dimethyl-6,7,9-trihydropyrido[1,2-*b*]acridine (1b). Following the procedure described for **1a**, 3,3′-dimethylcyclohexanone (147 mg, 1.16 mmol) was condensed with 8-amino-7-quinolinecarbaldehyde (200 mg, 1.16 mmol) in absolute EtOH (12 mL). The crude product was chromatographed on alumina (40 g), eluting with CH_2Cl_2/hexanes (1:1), followed by EtOAc/hexanes (1:1) to obtain **1b** (155 mg, 51%) as white crystals, mp 144−145 °C: ^{1}H NMR ($CDCl_3$) δ 9.20 (d, 1H, J = 3.0 Hz, H_9), 8.23 (d, 1H, J = 6.9 Hz, H_7), 7.95 (s, 1H, H_4), 7.70 (AB quartet, 2H, J = 2.4, 9.0 Hz, H_5/H_6), 7.60 (quartet, 1H, J = 3.6 Hz, H_8), 3.96 (broad s, H_2O), 3.19 (broad s, 2H, $-CH_2-$), 3.09 (t, 2H, J = 6.9 Hz, $-CH_2-$), 1.73 (t, 2H, J = 6.9 Hz, $-CH_2-$), 1.09 (s, 6H, CH_3); ^{13}C NMR ($CDCl_3$) δ 159.0, 150.0, 145.9, 144.2, 135.9, 135.3, 131.3, 128.2, 127.2, 126.2, 125.3, 122.4, 47.6, 35.4, 30.3, 28.2, 25.9. Anal. Calcd for $C_{18}H_{18}N_2 \cdot 0.25H_2O$: C, 81.06; H, 6.94; N, 10.51. Found: C, 81.21; H, 6.30; N, 10.44. MS *m*/*e* 262 (M^+).

4,6-Di(*p*-tolyl)-2-hydroxypyrimidine (6a). To urea (0.6 g, 9.5 mmol) dissolved in absolute EtOH (10 mL) were added 1,3-di(*p*-tolyl)-1,3-propanedione (1.2 g, 4.8 mmol) and concentrated HCl (1.2 mL), and the mixture was refluxed for 24 h. Additional urea (0.3 g, 4.7 mmol) and concentrated HCl (0.3 mL) were then added and the reflux continued for an additional 24 h. After cooling, the precipitate was filtered, washed with $CHCl_3$, triturated with hot acetone, and dried to yield **6a** (0.6 g, 46%) as a yellow powder, mp >270 °C: ^{1}H NMR (DMSO-d_6) δ 8.07 (d, 4H, J = 8.1 Hz, ArH), 7.60 (s, 1H, =CH−), 7.45 (d, 4H, J = 8.1 Hz, ArH), 4.80 (s, 1H, −OH), 2.42 (s, 6H, $-CH_3$).

4,6-Di(*p*-tolyl)-2-chloropyrimidine (6b). A mixture of **6a** (410 mg, 1.48 mmol) and *N*,*N*-dimethylaniline (3 drops) in $POCl_3$ (12 mL) was refluxed for 7 h. Excess $POCl_3$ was then removed by distillation under vacuum. The resulting oil was dissolved in cold water and extracted with CH_2Cl_2 (3 × 40 mL). The combined organic layers were dried over $MgSO_4$, concentrated, and chromatographed on alumina (25 g), eluting with CH_2Cl_2, to afford **6b** (100 mg, 23%) as a white solid, mp 142−145 °C: ^{1}H NMR ($CDCl_3$) δ 8.05 (d, 4H, J = 8.1 Hz, ArH), 7.96 (s, 1H, =CH−), 7.33 (d, 4H, J = 8.1 Hz, ArH), 2.44 (s, 6H, $-CH_3$).

4,4′,6,6′-Tetra(*p*-tolyl)-2,2′-bipyrimidine (2d). A mixture of anhydrous nickel chloride (89 mg, 0.68 mmol), triphenylphosphine (714 mg, 2.72 mmol), and zinc powder (63.5 mg, 0.97 mmol) was kept under Ar for 10 min. Freshly distilled DMF (4 mL) was then added, and the mixture was stirred at 50 °C for 30 min. To the dark red solution was added **6b** (200 mg, 0.68 mmol) in DMF (3 mL). Stirring was continued for 6 h at 50 °C. After cooling, the reaction mixture was poured into a mixture of NH_4OH (28−30%, 14 mL) and water (36 mL), stirred overnight, and extracted with CH_2Cl_2 (3 × 50 mL) in the presence of EDTA disodium salt (3 g) to break the emulsion. The organic layer was washed with water (30 mL), dried over $MgSO_4$, and concentrated. The resulting orange-yellow liquid was chromatographed on silica gel (25 g) eluting with hexane/EtOAc (4:1). Recrystallization from EtOH yielded **2d** (55 mg, 31%) as a white powder, mp 271−273 °C: ^{1}H NMR ($CDCl_3$) δ 8.25 (d, 8H, J = 8.1 Hz, ArH), 8.18 (s, 2H, =CH−), 7.38 (d, 8H, J = 7.8 Hz, ArH), 2.46 (s, 12H, $-CH_3$); ^{13}C NMR ($CDCl_3$) δ 165.8, 143.7, 141.2, 134.5, 129.6, 127.5, 111.7, 21.5. Anal. Calcd for $C_{36}H_{30}N_4 \cdot 1.5H_2O$: C, 79.27; H, 6.05; N, 10.28. Found: C, 79.37; H, 5.60; N, 10.15.

$[Cu(1a)_2]ClO_4$. Solid $[Cu(CH_3CN)_4]ClO_4$ (14 mg, 0.043 mmol) was added to a solution of **1a** (20 mg, 0.09 mmol) in CH_3CN (7 mL). The solution became dark red and was stirred at 25 °C under Ar for 1 h. The solution was concentrated under vacuum and the complex precipitated as air-stable, deep red crystals (22 mg, 81%): ^{1}H NMR (CD_3CN) δ 8.82 (broad s, 2H, H_9), 8.61 (d, 2H, J = 8.1 Hz, H_7), 8.33 (s, 2H, H_4), 8.03 (broad s, 4H, H_5/H_6), 7.84 (quartet, 2H, J = 4.8 Hz, H_8), 3.08 (t, 4H, J = 6.0 Hz, $-CH_2-$), 2.71 (broad s, 4H, $-CH_2-$), 2.19 (s, H_2O), 1.79 (broad s, 4H, $-CH_2-$), 1.67 (broad s, 4H, $-CH_2-$); MS *m*/*e* 529 $(M\text{-}ClO_4)^+$. Anal. Calcd for $C_{32}H_{28}N_4CuClO_4$: C, 60.87; H, 4.43; N, 8.88. Found: C, 60.84; H, 4.34; N, 8.70.

$[Cu(1b)_2]ClO_4$. Following the procedure described for $[Cu(\mathbf{1a})_2]ClO_4$, **1b** (50 mg, 0.2 mmol) was treated with $[Cu(CH_3CN)_4]ClO_4$ (31 mg, 0.09 mmol) in CH_3CN (7 mL) to give the complex as air-stable deep red crystals (57 mg, 92%): ^{1}H NMR (CD_3CN) δ 8.80 (d, 2H, J = 6.0 Hz, H_9), 8.64 (d, 2H, J = 6.0 Hz, H_7), 8.40 (s, 2H, H_4), 8.07 (broad s, 4H, H_5/H_6), 7.84 (quartet, 2H, H_8), 3.14 (t, 4H, $-CH_2-$), 2.46 (broad s, 4H, $-CH_2-$), 1.59 (t, 4H, $-CH_2-$), 0.65 (s, 12H, CH_3). Anal. Calcd for $C_{36}H_{36}N_4CuClO_4$: C, 62.90; H, 5.24; N, 8.15. Found: C, 62.79; H, 5.29; N, 7.80.

(20) Goulle, V.; Thummel, R. P. *Inorg. Chem.* **1990**, *29*, 1767.
(21) Bly, D. D. *J. Org. Chem.* **1964**, *29*, 943.
(22) Nasielski, J.; Standaert, A.; Nasielski-Hinkens, R. *Synth. Commun.* **1991**, *21*, 901.
(23) Choschi, T.; Horimoto, S.; Wang, C. Y.; Nagase, H.; Ichikawa, M.; Sugino, E.; Hibino, S. *Chem. Pharm. Bull.* **1992**, *40*, 1047.
(24) (a) Kubas, G. J.; Monzyk, B.; Crumbliss, A. L. *Inorg. Synth.* **1971**, *19*, 90. (b) Hemmerich, P.; Sigwart, C. *Experientia* **1963**, 488.

Table 4. Crystallographic Data for $[Cu(\mathbf{2c})_2](PF_6)$

chemical formula	$C_{64}H_{44}CuF_6N_8P$	fw	1133.58
a (Å)	14.761(2)	space group	*Pccn*
b (Å)	15.007(2)	T (°C)	−50
c (Å)	24.407(4)	λ (Å)	0.71073
α (deg)	90(1)	ρ_{calcd} (g cm^{-3})	1.393
β (deg)	90(1)	μ (cm^{-1})	5.04
γ (deg)	90(1)	R1[a]	0.0436
V (Å^3)	5406.8(14)	wR2[b]	0.1145
Z	4		

[a] $\sum||F_o| - |F_c||/\sum|F_o|$. [b] $[\sum w(F_o^2 - F_c^2)^2/\sum w(F_o^2)^2]$; $w = [(F_o^2) + (0.0566P)^2 + (6.77P)]^{-1}$, where $P = (F_o^2 + 2F_c^2)/3$.

$[Cu(2b)_2]PF_6$. To a solution of **2b** (103 mg, 0.48 mmol) in CH_3CN (20 mL) was added $[Cu(CH_3CN)_4]PF_6$ (89.2 mg, 0.24 mmol), and the mixture was stirred for 1 h. The solvent was concentrated, and the precipitate was dried overnight to provide $[Cu(\mathbf{2b})_2]PF_6$ as a red solid (137.2 mg, 90%): ^{1}H NMR (CD_3CN) δ 7.47 (s, 4 H, ═CH), 2.45 (s, 24 H, CH_3). Anal. Calcd for $C_{24}H_{28}N_8CuPF_6 \cdot 0.25H_2O$: C, 44.94; H, 4.44; N, 17.47. Found: C, 45.30; H, 4.43; N, 17.06.

$[Cu(2c)_2]PF_6$. A solution of **2c** (52.1 mg, 0.113 mmol) in CH_3CN (15 mL) was gently warmed to ensure the complete dissolution of the ligand. Solid $[Cu(CH_3CN)_4]PF_6$ (21 mg, 0.056 mmol) was then added, and the dark solution was stirred at room temperature for 1 h. Concentration under vacuum gave $[Cu(\mathbf{2c})_2]PF_6$ as an air-stable dark purple solid (67 mg, 93%): ^{1}H NMR (CD_3CN) δ 8.16 (bs, 20H, ArH and ═CH−), 7.42 (bs, 24H, ArH). Anal. Calcd for $C_{64}H_{44}N_8CuPF_6 \cdot H_2O$: C, 66.77; H, 4.00; N, 9.73. Found: C, 66.60; H, 3.90; N, 10.12.

$[Cu(2d)_2]PF_6$. A solution of **2d** (41.1 mg, 0.08 mmol) in CH_3CN (10 mL) and CH_2Cl_2 (5 mL) was gently warmed to ensure the complete dissolution of the ligand. Solid $[Cu(CH_3CN)_4]PF_6$ (14.74 mg, 0.04 mmol) was then added, and the dark purple solution was stirred at room temperature for 2 h. Concentration under vacuum gave $[Cu(\mathbf{2d})_2]PF_6$ as an air-stable purple solid (45 mg, 91%): ^{1}H NMR ($CDCl_3$) δ 8.20 (bs, 8H, ArH), 7.70 (s, 4H, ═CH−), 7.63 (bs, 8H, ArH), 7.37 (bs, 8H, ArH), 6.75 (bs, 8H, ArH), 2.44 (bs, 12H, $-CH_3$), 1.68 (bs, 12H, $-CH_3$). Insufficient sample was available for CHN analysis.

Crystal Structure Determination of $[Cu(2c)_2](PF_6)$. A red-orange thick plate having approximate dimensions 0.15 × 0.25 × 0.35 mm was mounted in a random orientation on a Nicolet R3m/V automatic diffractometer. The sample was placed in a stream of dry nitrogen gas at −50 °C, and the radiation used was Mo Kα monochromatized by a highly ordered graphite crystal. Final cell constants, as well as other information pertinent to data collection and refinement, are listed in Table 4. The Laue symmetry was determined to be *mmm*, and from the systematic absences noted the space group was shown unambiguously to be *Pccn*. Intensities were measured using the ω-scan technique, with the scan rate depending on the count obtained in rapid prescans of each reflection. Two standard reflections were monitored after every 2 h or every 100 data collected, and these showed no significant variation. During data reduction Lorentz and polarization corrections were applied; however, no correction for absorption was made due to the small absorption coefficient.

The structure was solved by the SHELXTL direct methods program, which revealed the positions of most of the non-hydrogen atoms in the molecule. Remaining atoms were located in subsequent difference Fourier syntheses. The usual sequence of isotropic and anisotropic refinement was followed, after which all of the hydrogens were entered in ideal calculated positions and constrained to riding motion, with a single variable isotropic temperature factor for all of them. After all shift/esd ratios were less than 0.1, convergence was reached at the agreement factors listed in Table 4. No unusually high correlations were noted between any of the variables in the last cycle of full-matrix least-squares refinement, and the final difference density map showed a maximum peak of about 0.45 e/Å^3. All calculations were made using Bruker's SHELXS-97 (Sheldrick, 1997) series of crystallographic programs.[25]

Acknowledgment. We would like to thank the Robert A. Welch Foundation (E-621), the National Science Foundation (CHE-9714998), and the Petroleum Research Fund of the American Chemical Society for financial support of this work. We would also like to thank Dr. James Korp for assistance with the X-ray determination, Julien Wellhoff for assistance with the electrochemical measurements, and Dr. Debby Roberts for assistance with the mass spectrometry.

Supporting Information Available: Tables of atomic coordinates, bond lengths, bond angles, anisotropic displacement parameters, and H-atom coordinates for $[Cu(\mathbf{2c})_2](PF_6)$; VT NMR data used to determine the kinetic parameters outlined in Table 1. This material is available free of charge via the Internet at http://pubs.acs.org.

IC0000606

(25) Sheldrick, G. M. In *Crystallographic Computing 3*; Sheldrick, G. M., Kruger, C., Goddard, R., Eds.; Oxford University Press: Oxford, U.K., 1985; pp 175−189.